

Intra-Cavity Adaptive Optics Control of 1 μ m Solid-State Lasers

W. Lubeigt, G.J. Valentine and D. Burns
Institute of Photonics, University of Strathclyde,
106 Rottenrow
Glasgow, G4 0NW

Abstract

An intra-cavity deformable membrane mirror (DMM) has been used to optimise the brightness of a 15W, diode-pumped, grazing incidence Nd:GdVO₄ laser. In one configuration an order of magnitude improvement of laser beam quality was recorded with negligible drop in output power. Local and global optimum-locating algorithms have been developed to enable automatic optimisation of the laser quality, and have been tested in both intra- and extra-cavity configurations. A novel laser brightness sensor based on second-harmonic-generation has also been developed to assess the progress of the laser towards optimisation. A tip & tilt mirror was also incorporated in the laser resonator cavity in order to enhance the optimisation capabilities.

Keywords: Solid-state laser, spatial mode, thermal effects, adaptive optics, second-harmonic-generation

Introduction

Thermally induced aberrations are one of the main impediments to be overcome in developing high-power solid-state lasers [1]. These aberrations, induced by the substantial heat loading, severely limit the transverse mode quality in high average power laser systems [2].

Thermal lensing and thermally induced birefringence within the gain material can significantly affect the stability and efficiency of the laser, however, through good design these can, in general, be controlled. Effective elimination of thermally induced birefringence results through use of a naturally birefringent laser crystal, or by exploiting a polarisation insensitive laser cavity configuration [3]. The spherical component of the thermal lens can also be compensated and controlled [4], however, typically only over a small range of absorbed pump powers. Unfortunately, there is no simple, effective means of compensating

against the effects of the non-spherical component of the induced thermal lens. The goal of this work is therefore to investigate the potential of using intra-cavity adaptive optics techniques as a general vehicle for thermal aberration correction over a wide operating range, and so, extend the potential of high power solid state lasers.

Our initial studies demonstrated the potential for spatial mode enhancement by using an intra-cavity adaptive optics element [5], [6] where (as shown in figure 1) a 15mm diameter OKOTECH deformable membrane mirror (DMM) [7] was operated in a computer-controlled, self-optimisation, feedback scheme.

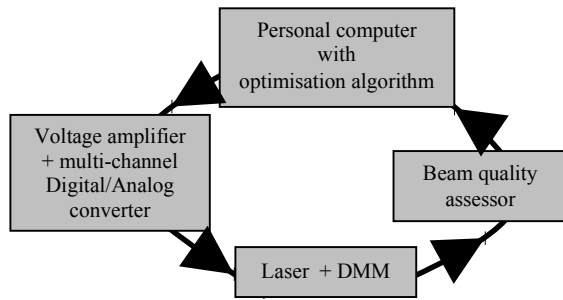


Fig. 1. Closed-loop intra-cavity adaptive optics optimisation scheme

In this system, the laser output was detected by a beam quality assessor to determine a so-called ‘fitness’ value, which is then sent to the optimisation algorithm. The term ‘fitness’ is used to describe the operational performance of a particular laser parameter, for example, the output transverse mode quality. [A much superior measure of laser performance is brightness, as this reflects both the beam quality and total output power, and is the fitness measure used throughout this work.]. The computer controls the shape of the intra-cavity DMM via a combined digital-to-analog converter (DAC) and voltage amplifier unit. The automatic optimisation scheme is then completed by employing a suitable control algorithm.

In this paper, the different components of this adaptive control system will be discussed in detail. In the first section, a description of the laser quality assessor will be given; optimisation algorithm development will then be detailed; then, finally, the practical optimisation of a Nd-based laser will be discussed.

Second-harmonic generation-based brightness sensor

One of the crucial elements in the intra-cavity adaptive optics optimisation procedure is to determine how well the laser is operating. To assess this, we use the concept of a fitness parameter which reflects the particular performance metric to be optimised. In our work to date, only the spatial mode quality of the laser has been addressed, however, these techniques should be readily applicable to other laser properties. As stated above, with regard to high average power lasers, a

measure of the output brightness would be most desirable. However, a conventional laser brightness monitor is not altogether straightforward, being either time consuming or expensive. Fortunately, for adaptive optics (AO) control only a qualitative measurement is required, i.e. the fitness parameter should increase/decrease as the brightness increases/decreases. This then, can lead to a much simpler, cost-effective, real-time brightness sensor.

The brightness of a light source is defined as the power (P) emitted per unit surface area (A) per unit solid angle (Ω) [2]:

$$B = \frac{P}{A\Omega} \quad (1)$$

Also, the most commonly expressed parameter used to define the quality of a laser beam is the so-called beam quality factor, generally referred to as M^2 and defined as:

$$M^2 = \frac{\pi\Theta\omega}{\lambda} \geq 1 \quad (2)$$

where Θ is the divergence angle (at a distance much larger than the Rayleigh Length) and ω the width of the beam waist.

So, by expressing the ‘area’ of the laser beam as $A=\pi\omega^2$, and the subtended solid angle as $\Omega=\pi\Theta^2$, we can obtain, by combining equations (1) and (2), an expression for brightness containing only our laser parameters:

$$B = \frac{P}{M^4\lambda^2} \quad (3)$$

All these expressions are valid for a circular cross-section laser beam, however, for the more general case of elliptical beams, the relation:

$$M^4 = M_x^2 M_y^2 \quad (4)$$

can be used. Where M_x^2 and M_y^2 are the corresponding beam quality factors in the x and y directions respectively.

Consequently, the brightness of a laser beam can be defined simply in terms of the beam quality parameters, M_x^2 , M_y^2 , and the output power, P:

$$B = \frac{P}{M_x^2 M_y^2 \lambda^2} \quad (5)$$

The brightness can be seen to increase as the power increases, and also as the beam quality (of each or both orthogonal planes) is enhanced. So, a qualitative brightness sensor must be sensitive to both power and beam quality changes.

It is well known that the efficiency of driving nonlinear optical effects generally improves as beam power and quality increase (at least for volumetric effects). We therefore decided to implement a second harmonic generation (SHG) [8] crystal to derive our brightness-based laser fitness parameter. A simple schematic (shown in figure 2) describes this sensor, for two input laser beams having the same average power. As the intensity of the brighter incident beam is maintained throughout the SHG crystal a significantly larger SHG output is produced. This dependence of the SHG conversion efficiency on the beam quality parameter M^2 can be calculated, and is shown figure 3 for a 20mm KTP crystal. [In this calculation the focussing was optimised for a fundamental Gaussian beam ($M^2=1$), i.e. Rayleigh range ~ 10 mm.]

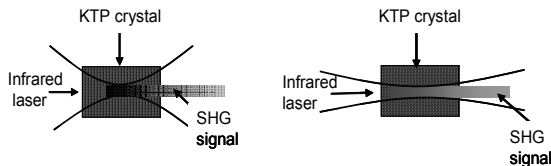


Fig. 2. SHG for two laser beams of the same power but different brightness (low – LHS, high – RHS)

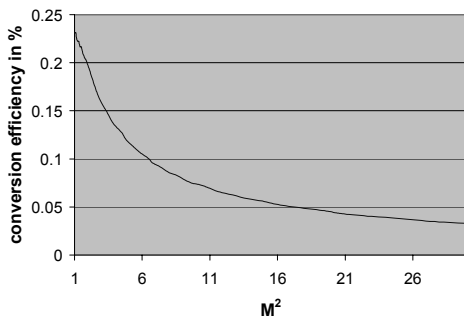


Fig. 3. Influence of the beam quality parameter on the SHG efficiency in a 20mm KTP crystal

The SHG conversion efficiency is strongly dependent on the M^2 for values of less than about 15, however, for higher M^2 values the conversion efficiency changes at a much reduced rate. It is clear then that SHG is a sensitive measure of laser beam quality, and becomes much more so as the laser approaches its ultimate performance.

Additionally, as is well known, the second harmonic power, $P_{2\omega}$, is also quadratically dependent on the incident fundamental power, P_{ω} [9] via the relation:

$$P_{2\omega} = \gamma_{sh} P_{\omega}^2 \quad (6)$$

where γ_{sh} is the SHG conversion efficiency.

Thus, using equation (5) and considering that the SHG power is quadratically dependent of the fundamental power and that the SHG conversion efficiency is strongly dependent on the beam quality of the fundamental beam, a brightness assessment based on SHG should be an efficient brightness sensing technique.

The experimental set-up of the sensor is shown schematically in figure 4, where the laser output is focussed onto a 20mm long KTP crystal using an $f=45$ mm lens. The infrared light is then filtered out using a harmonic separator designed for 1064/532nm such that only the resultant SHG signal is recorded by the photodetector. The detected SHG signal then represents a measure of the laser beam brightness, and is fed to the pc hosting the control algorithm via the analogue input of our PICDAC electronics interface.

The KTP crystal was mounted onto a dual rotational axis mirror mount in order to improve the conversion efficiency, however, once aligned no further adjustments were necessary.

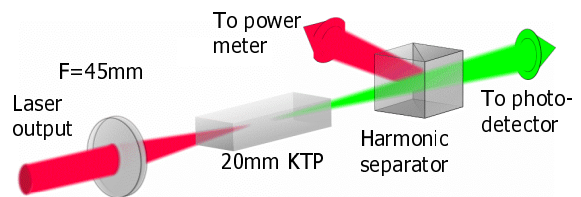


Fig. 4. Experimental set-up of the SHG-based laser brightness sensor

The development of an SHG-based brightness assessment technique provides several advantages with regard to AO control of lasers: Firstly, the sensor system does not require any electronics which provides a significant improvement in simplicity and cost of the system. Additionally, no power-meter/monitor is required, and only a simple photodiode is necessary to measure the intensity of the SHG signal. The limitation of reduced sensitivity to beam quality at high M^2 values is a remaining issue, however, in our studies this was not an obvious shortcoming. Further refinements of our system will include a boxed prototype to mitigate alignment issues, increase ruggedness, and limit any crystal damage from mechanical shock or water ingress.

As implied in figure 3, no significant loss of output power occurs as the highest conversion efficiency in the crystal did not exceed 0.25%, so the sensor is appropriate for use with the full laser output. The focal length of the focussing lens can then be chosen appropriately depending on the power of the laser system, providing good quality sensor information without fear of SHG crystal damage.

Optimisation algorithms

Another critical element of the closed-loop adaptive optics scheme developed here was the algorithm used to control the progress of the optimisation sequence. The algorithm controls the voltages applied to the mirror transducers, and hence its shape, dependent on the input fitness values. As, in this case, the shape of the deformable membrane mirror is determined by the voltages applied (0-200V) to each of the 37 electro-static actuators, we then have $>10^{89}$ different possible solutions for an 8-bit voltage resolution. Such a vast potential search space, coupled with a desire for fast and efficient optimisation, then implies the choice of the algorithm is a fundamental concern.

Of search algorithms appropriate to our laser development, some algorithms (e.g. the hill-

climbing algorithm) can only typically locate a local optimum, with the solution found being dependent on the starting point of the optimisation. However, other algorithms such as the genetic algorithm (GA), random search (RS), adaptive random search (ARS) and simulated annealing (SA) can locate the global optimum solution without interference from the starting point of the optimisation procedure. These algorithms are very different in their behaviour in that they are stochastic or non-deterministic search techniques essentially based on random jumps throughout the whole search space. This nature is in contrast to more direct algorithms (e.g. hill-climbing) which are deterministic in their behaviour and as such, are completely predictable given knowledge of the starting point.

The most straight-forward algorithm deployed in this work was a modified hill-climbing algorithm (MHC). The modification, deployed for coding simplicity, allowed the algorithm to find the maximum of each axis of the search space in turn, instead of following the gradient of the local region of the search space. The MHC was, as expected very efficient and fast, however, the inability to locate the global maximum was a clear drawback. [A full description of the MHC was given in last year's report [5].] This inadequacy led to the development and implementation of a range of more advanced non-deterministic algorithms.

One such procedure, the Genetic Algorithm (GA) [5, 10], was developed to ensure that the global maximum was always returned by the optimisation process. The GA is closely based on the principles of Darwinian natural selection [11], and a full description can be found in [5]. The GA, albeit a little slow, works well, however, issues specifically relating to the time taken to reach an equilibrium state in high average power 'hot' lasers, implied that further algorithm development was necessary. To this end, we considered the so-called 'simulated annealing'

algorithm to enhance the speed of the optimisation process.

The simulated annealing algorithm

Simulated annealing employs a Monte-Carlo approach to find solutions of multi-variate/multi-dimensional problems. The Monte-Carlo method provides approximate solutions to a variety of mathematical problems by performing statistical sampling experiments on a computer [12, 13]. In 1983, Kirkpatrick and coworkers proposed the simulated annealing optimisation scheme based on the Metropolis Monte Carlo method to find the most stable orientation of a system [14].

The simulated annealing algorithm, not surprisingly, is analogous to the physical process of annealing, i.e. heating followed by slow cooling to eliminate defects and dislocations, and so, improve the crystalline structure of solids. The algorithm progressively, but slowly, lowers the ‘temperature’ allowing the system to re-configure into a more optimal state. [The concept of temperature in the algorithm is obviously abstract. It relates to degree of perturbation allowed, and the probability of a new state being chosen over an existing state.] At ‘high temperatures’ the system is allowed to change by a large extent such that the whole solution space can be searched, whereas, as the temperature lowers, only progressively smaller changes are allowed. The system temperature is also used in calculating the probability of accepting a new state having a lower fitness value. This process continues until the system ‘freezes’ and no further changes occur.

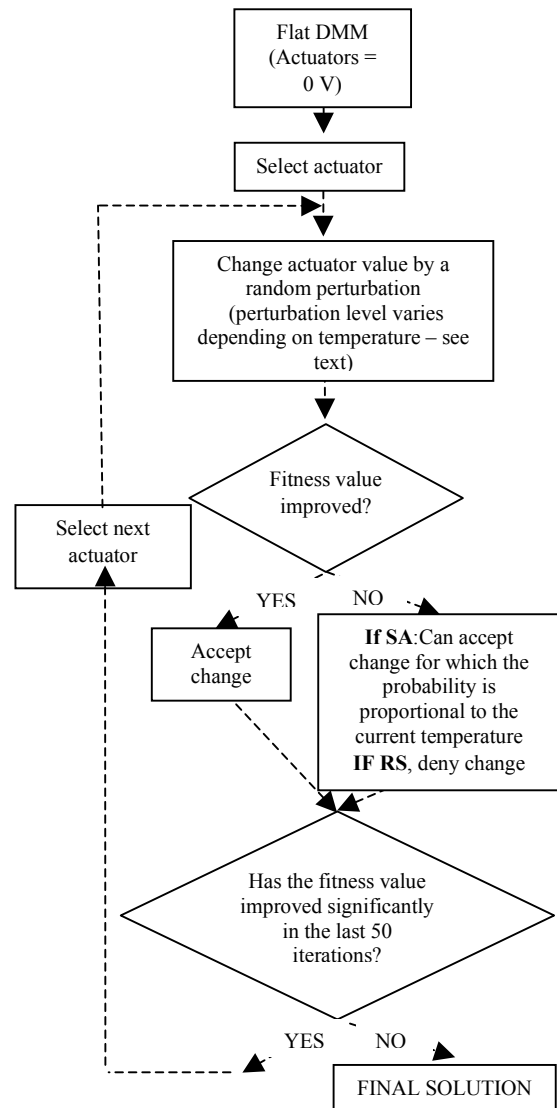


Fig. 5: Flowchart of the RS and SA algorithm.

The simulated annealing algorithm samples the search space in a completely different way (see the flowchart in figure 5) than the GA, and can return the optimum result much faster [15]. With regard to laser cavity optimisation, the SA has the significant advantage that only relatively small mirror shape changes are involved. This important feature allows for faster searching and, as will be discussed more fully later, a reduced tendency for modal collapse.

The random and adaptive random search algorithms

As mentioned above, the SA can accept intermediate solutions having lower fitness than preceding states during the search. This feature, controlled by the Metropolis value

and the system temperature, helps the SA to avoid being trapped at a local maximum within the search space, and so allow the true optimum solution to be found. This does require a certain amount of calibration which can pose some practical problems, however, if we impose the restriction that a state change can only occur if the fitness is improved then the SA reduces to two new algorithms – the random search (RS) and adaptive random search (ARS) algorithms. [In practice, this reduction is done simply by selecting a large Metropolis value.]

The RS (see figure 5) and ARS algorithms are very similar, however the ARS takes into account the notion of temperature in a similar way as the SA. This has the effect of reducing the magnitude of the search as the algorithm progresses, unlike in RS where the perturbation is kept fixed and equal to the magnitude of each axis of the search space. Therefore, the RS continues to search the full bounds of each axis for the duration of the optimisation, whereas the ARS continually narrows its focus, a property that can lead to undesirable results. In general, we have found that the narrowing focus of the ARS makes it of very limited benefit for laser optimisation, however, and perhaps surprisingly, the RS algorithm may be deemed to be the best all-round optimisation technique for laser brightness optimisation (a fact the belies that it cannot, in principle, be considered to be a global optimisation method).

Preliminary comparison of search algorithms

To test and compare the different algorithms developed here a simulated multi-dimensional space encoded by way of an embedded test function within the optimisation software was exploited. The RS, ARS, SA and GA were the then set to find the global maximum solution of this space (which resided at a position where all 37 actuators had a value of 3776 in a 12-bit parabolic space giving a fitness value equal to 190.6).

The GA, SA and RS returned the global maximum value, however, the GA was clearly

the most inefficient in terms of optimisation speed. The SA and RS efficiently returned the best possible solution in around 8500 samples in comparison to the 10^{89} possible combinations. [N.B. the axes of the test space were nonlinear, having 256 values, each coded to a 12-bit accuracy. This was used to linearise the response of the deformable mirror.) The ARS consistently failed to reach the global maximum value.

In general, it can be noted that for any space search, the GA will always, in time, find the global maximum. The SA will also, in principle, perform well provided appropriate calibration of the cooling rate and Metropolis value are used. However, this calibration can be tedious and difficult. The RS almost always reaches the global maximum, but can terminate on a local maximum in certain cases depending on the complexity of the search space. Table 1 summarises the performance of the algorithms determined from the test function optimisation procedure. The column termed ‘number of samples’ indicates the average number of times the algorithm examines the search space as it progresses towards a final solution.

Algorithm	Fitness value reached	Number of samples
GA	188	300 000
RS	188	8000
ARS	32.1	3500
SA	188	9000

Table 1: optimisation results summary

Comparison of the algorithms using an adaptive confocal microscopy system

A deformable membrane mirror was introduced into a confocal microscope system in order to reduce the sample induced aberrations. This method represented a real practical test-bed for assessing the various AO techniques developed (the simulated annealing algorithm was not initially deployed in this set-up).

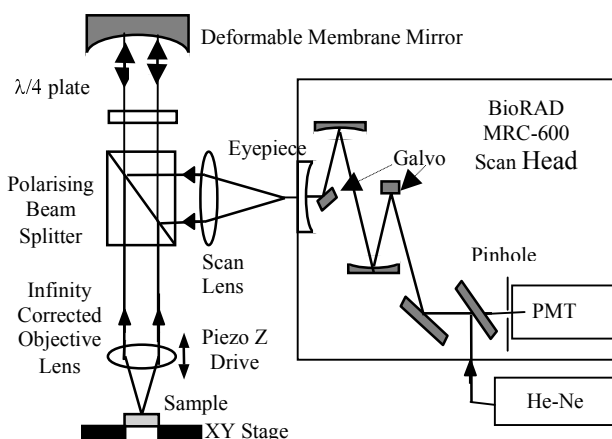


Fig. 6: The AO confocal microscope

The AO microscope system is reproduced in figure 6. Here, a 2mW Helium Neon (633nm) laser beam was directed into a MRC-600 BioRad scan head. The output from the scan head was then directed via a polarizing beam splitter cube and a quarter wave plate towards a deformable membrane mirror (DMM). The light reflected off the DMM was focused using a Nikon (0.5N.A. x20) microscope objective onto the test sample. Even at this relatively low N.A., aberrations induced when imaging at depth significantly degrade the image quality (see figure 7). The return signal from the sample reached the pinhole and photomultiplier tube (PMT) via a second pass on the DMM.

The test sample consisted of various depths of water sandwiched between a standard glass microscope cover slip and an enhanced aluminium mirror. Using these test samples, as opposed to using a real biological test samples, it was possible to accurately control and assess the sample aberrations.

A piezoelectric transducer (PZT) controlled the position of the microscope objective in the z-direction. In this way, the axial point-spread-function (PSF), and hence the axial resolution of the system, could be recorded by scanning the microscope objective in the z-direction whilst recording the intensity of the reflected beam detected by the PMT. This process was automated and resultant fitting to a Gaussian distribution determined the PSF of the system. The axial resolution, Δz , was then calculated [16] using the relation:

$$\Delta z = 1.2 \times PSF_{FWHM} \quad (5)$$

To optimise the performance of this system an analogue signal was derived by ‘parking’ the z-translation such that the signal at the PMT was maximised. This value was then used as the fitness value in the optimisation control algorithm. A highly aberrated PSF can contain more than one peak of equal amplitude and it is essential to the success of the optimisation that the correct peak is selected. When this situation arose preliminary optimisations using the hill climbing algorithm were used to determine the most appropriate peak.

For each sample, an initial PSF was recorded with 0V on all the DMM actuators (see figure 7). The system was then optimised and direct measurement of the axial PSF was used to assess the success of each optimisation algorithm after completion. In addition, a sample containing no water, and therefore no sample aberrations, was measured to give a baseline resolution for the optical system. Figure 7 summarises the results of these experiments.

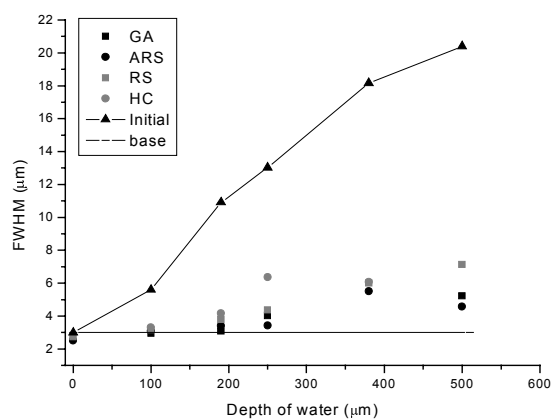


Fig. 7: Improvement in the resolution of a confocal microscope system using AO optimisation

Even when using the basic MHC algorithm, the axial resolution of the system was reduced by at least factor of 1.7 compared to that measured without any optimisation. This resolution enhancement factor increased up to 4.5 when other algorithms, in particular the ARS or the GA, were used. Although the

MHC often returned a similar result to the other algorithms, the data recorded using 250 μ m of water illustrates a situation where the MHC algorithm has located a local maximum solution rather than the desired global maximum solution.

The optimisation software was designed with an intensive graphical interface to provide a continuous diagnostic for the user which significantly extended the time taken to run all the algorithms. For example, the efficient RS algorithm reached a solution in the range 2-7 minutes. However, software refinement, specifically through reducing the graphics intensive interface these times could, in principle, be significantly reduced. For example, for the RS, a typical optimisation may consist of ~8000 trials, which could be translated to an optimisation time of a few seconds, bottlenecked primarily by the bandwidth of the AO mirror.

A comparison and commentary of the four different algorithms when using a 250 water sample is shown in table 2 below.

Algorithm	Input parameters	Time to complete	Axial enhancement factor	Comments
MHC	- Voltage range - Voltage step size - Actuator order	48s (fast)	3.3 – 2.2	Ideal for quick trial optimisation
GA	- Cross over - Mutation - Stopping condition	3m 50s-12m 32s (very slow)	3.8 – 3.5	achieves 'ultimate' solution if left long enough.
RS	- Stopping condition - Actuator order	2m 27s – 6m 17s (slightly slow)	3.9 – 3.5	Best all round option.
ARS	- Stopping condition - Rate of decrease in perturbation - Actuator order	3m 1s – 10m 16s (relatively slow)	3.7 – 2.9	no benefits over the RS.

Table 2: Results summary of AO microscope

Experimental laser cavity set-up

AO optimisation of a multi-mode laser

To fully investigate the potential of an intra-cavity deformable mirror to optimise the modal performance of an all-solid-state laser, the diode-pumped, grazing-incidence Nd:GdVO₄ resonator as shown in figure 8

was configured. This set-up maximises the induced aberrations for a given pumping power, and so, was considered an appropriate test-bed for our AO optimisation studies.

The incident pump power was derived from two spatially coupled diode bars giving a total power up to 50W. A 50% output coupler was used throughout as this was found to give optimum performance under these pumping conditions. The incorporation of an x6 intra-cavity telescope relayed a large (~8mm diameter) spot onto the deformable mirror, and so, good overlap with the underlying actuator array was ensured. This magnification also acted to enhance the effect of the reconfigurable deformable mirror on laser operation.

Using the GA and the SHG-based mode quality sensor described earlier, an optimisation routine was performed with 50W incident pump power. This optimisation routine lasted about 15 minutes, during which the output power slightly decreased from 15W to 14W. However, on measurement of the beam propagation parameter M^2 , in the tangential plane a decrease from 27 to 9, and in the sagittal plane a decrease from 10.5 to 3 were recorded. The near-field and far-field distributions of the output beam before and after optimisation are shown respectively in figures 9 and 10.

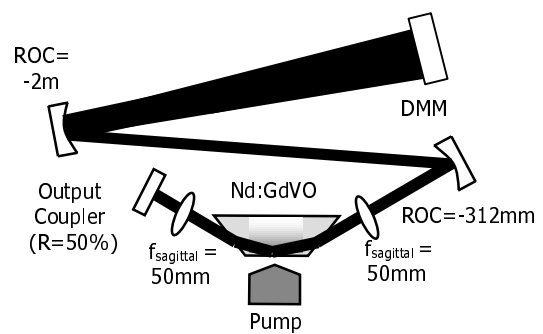


Fig. 8. Experimental AO laser set-up

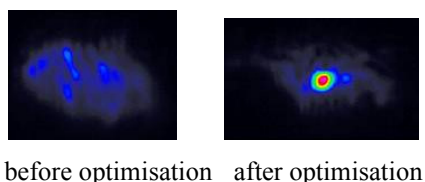


Fig. 9. Near-field beam profiles

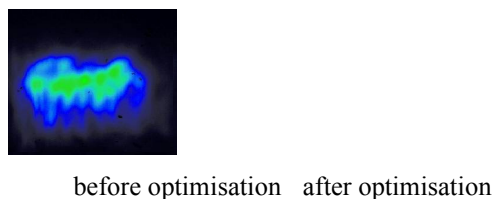


Fig. 10. Far-field beam profiles

Therefore, the automatic AO optimisation scheme employed successfully increased the laser mode quality by approximately 3 times in each axis while maintaining a consistent average laser output power of $\sim 15\text{W}$, which translates to an order of magnitude enhancement in brightness.

Stability issues, reproducibility, the influence of noise (both optical and electrical), and the limitations on the induced enhancement became relevant during these experiments, and it is these topics that will now be addressed.

Development of a large- mode laser

It was apparent from the optimisation of the 15W Nd:GVO₄ laser that the possible enhancement in the brightness will be related to the overlap of the fundamental mode with the pumped volume within the gain medium. The mode distribution within the laser rod configures to efficiently extract the available gain, and so, the basic shape of the pumped region is transferred to the oscillating mode profile. If the resonator is configured to give a small relative fundamental mode area, then a substantial higher-order mode content is required to ‘fill-in’ the regions of un-used gain in the laser rod. So, in this case, (without resorting to using apertures which will reduce the modal content of the output but at the expense of total power) brightness enhancement will be limited to that induced by the subtle modal reconfiguration made possible by deformable mirror. Our attention

then turned to the other extreme case, i.e. where the fundamental mode is ‘matched’ to the pumped region, to examine the benefits, or otherwise of AO optimisation.

The laser cavity in figure 8 had a fundamental mode radius of $\sim 300\mu\text{m}$ in the tangential plane. And since the majority of the incident pump was absorbed within the first 2mm of the crystal surface, the highly multimode oscillation in the tangential plane was to be expected. To enlarge the fundamental mode radius to $\sim 1\text{mm}$ within the gain medium, the cavity was reconfigured by extending the short cavity arm (as shown in figure 8) and adjusting the cylindrical lens to re-establish resonator stability. This cavity did indeed exhibit single transverse mode oscillation (see figure 11), however, the output power was significantly reduced to $\sim 4\text{W}$ for an incident pump power of 40W .

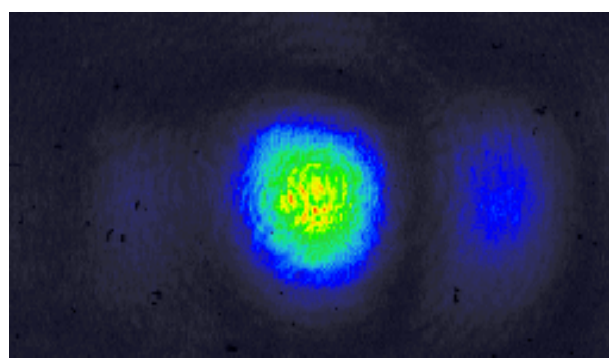


Fig. 11. Beam profile

Results obtained from the optimisation of this low-order mode laser using our algorithms suite are shown below in table 3.

	Start of optimisation	End of GA	End of RS	End of ARS	End of SA
Fitness	170	360	360	360	360
Power	3.7W	4.3W	4.3W	4.3W	4.1W
No. of mirror changes		1600	550	550	550

Table 3. Comparison of tailored algorithms in the brightness enhancement of an Nd:YVO₄ laser

Again, the GA, RS and ARS reached the same optimum result but the GA used about 3 times more resources. The SA required some tuning

of the calibrating Metropolis value, however, after this was achieved, good performance resulted. It was clear that the degree of performance enhancement was not as dramatic as for the multi-mode laser case, however, these results are somewhat provisional and more investigation is required to fully assess the benefits of such large-mode laser configurations.

Tailored algorithms and implementation of tip/tilt alignment capability

When working with ‘hot’ distorted gain media, a few practical issues become immediately evident and require attention, these are:

- i. thermal lag
- ii. noise, both electrical optical, and
- iii. modal collapse

i. The thermal lag issue simply manifests as a limitation to the speed of the optimisation procedure, which, of course, has implications to the practical application of this technology but does not in itself limit the potential laser performance enhancements that can be induced. In practice, a user settable delay between the application of a mirror change and the measurement of the effects induced is used to account for this lag. Control algorithms where sequences of small changes are used to search for the optimal solution (e.g. SA and RS) induce only minimal lag and so can significantly speed up the optimisation.

ii. Fluctuations in output power cause a much more serious problem specifically in the context of the use of evolutionary algorithm control of lasers. Simply put, the evolutionary process is driven by a comparison of a single valued parameter for each sampled state of the laser, and noise can significantly mess up this selection process. In our system, signal averaging is employed to reduce these effects, however, such averaging cannot compensate for slow passive optical drift over time. We then must ensure that the passive laser platform possesses a high degree of long-term stability to make certain of good optimisation

success. However, during these developmental phases this is not always possible, and so, modifications to the algorithms have been made to account for this problem. Firstly, in the GA, the fitness of the previously best solution is re-tested each generation such that its comparison to new solutions is still valid. Also similarly, in ARS, RS and SA cases the current best mirror shape has its fitness re-measured at the end of each cycle. The effect of these modifications is that the search for the optimal solution can still be maintained even if mechanical or environmental factors cause the average output power to vary.

iii. The issue of modal collapse due to large optical changes is perhaps the most serious problem, and can completely ruin any attempts to optimise the laser via the techniques developed here (apart maybe, from a true hill-climbing approach). The RS, ARS or SA reduce the probability of modal collapse as the change of mirror shape is small with only one actuator being changed at any one time, however, the GA with its full 37 transducer variations has very little chance of success.

The specific difficulty with the effect we term ‘modal collapse’ is that it is non-reversible. If induced, then simply resetting the previous cavity or mirror settings will not, in general, re-establish the previous oscillation state. At present, there is no obvious solution to mitigate the effects of modal collapse apart from using the ‘gentler’ algorithmic approaches such as SA and RS.

Further to these modifications designed to address specific ‘hot’ laser related problems, we have extended the potential for greater degrees of optimisation by incorporating a piezo-electric tip/tilt mirror into the laser resonator. The tip and tilt functions were integrated easily into the control scheme as these were considered simply as two extra actuators in the algorithm process. Extension of this tip/tilt function to more than one mirror shows promise for active laser alignment to complement the active optimisation already

demonstrated.

Future Work

In the next year, we plan to further develop the control algorithms by tailoring them to better suit the problem being investigated. This tailoring process will account for effects such as; noise, thermal drift/lag, and the use of reduced search fields.

The tip/tilt capability will also be improved by using a set of two tip/tilt mirrors in the laser resonator in order to obtain a 'beam walking' scenario.

Acknowledgments

The work reported in this paper was funded by the Electro-Magnetic Remote Sensing (EMRS) Defence Technology Centre, established by the UK Ministry of Defence.

References

1. J.M. Eggleston, T.J. Kane, K. Kuhn, J. Unternahrer, and R.L. Byer, "The slab geometry laser. I. Theory," IEEE J. Quantum Electron., **QE-20**, pp. 289-301, 1984
2. W. Koechner, *Solid-State Laser Engineering*, 5th edition (Springer Series in Optical Sciences, 1999)
3. W.A. Clarkson, N.S. Felgate, D.C. Hanna, "Simple method for reducing the depolarization loss resulting from thermally induced birefringence in solid-state lasers," Opt. Lett. **24**, pp. 820-822 1999
4. D. Burns, G.J. Valentine, W. Lubeigt, E. Bente, A.I. Ferguson, "Development of High Average Power Picosecond Laser Systems," Proc SPIE **4629**, pp. 4629-18, 2002
5. W. Lubeigt, P. Van Grol, G. J. Valentine and D. Burns, "Use of intra-cavity adaptive optics in solid-state lasers operating at 1 μ m", ERMS DTC 1st annual technical conference, 2004
6. W. Lubeigt, G. Valentine, J. Girkin, E. Bente, and D. Burns, "Active transverse mode control and optimisation of an all-solid-state laser using an intracavity adaptive-optic mirror," Opt. Express **10**, 550-555, 2002,

<http://www.opticsexpress.org/abstract.cfm?URI=OPEX-10-13-550>

7. Flexible Optical B.V., PO Box 581, 2600 AN, Delft, the Netherlands, www.okotech.com
8. G. D. Boyd and D. A. Kleinman, "Parametric interaction of focused Gaussian light beams," J. Appl. Phys. **39** (8), pp. 3597-3639, 1968
9. W. J. Kozlovsky, C. D. Nabors and R. L. Byer, "Efficient second harmonic generation of a diode-laser-pumped CW Nd:YAG laser using monolithic MgO:LiNbO₃ external resonant cavities," IEEE J. Q. Electron. **24** (6), pp. 913-919, 1988
10. K.F. Man, *Genetic Algorithm: Concept and Designs*, (Springer Series, 1999)
11. C. Darwin, *On the origin of species by means of natural selection*, (J. Murray, London, 1859)
12. N. Metropolis and S. Ulam, "The Monte Carlo Method," J. Amer. Stat. Assoc. **44**, pp. 335-341, 1949
13. N. Metropolis, A.W. Rosenbluth, M.N. Rosenbluth, A.H. Teller and E. Teller, "Equation of State Calculations by Fast Computing Machines," J. Chem. Phys. **21**, pp. 1087-1092, 1953
14. S. Kirkpatrick, C.D. Gelatt and M.P. Vecchi, "Optimization by simulated annealing," Science **220**, pp. 671-680, 1983
15. "Empirical comparison of stochastic algorithms," in *Proceedings of the Second Nordic Workshop on Genetic Algorithms and their Applications*, (T. Jarmo, Alander, Finland, 1996), <http://www.uwasa.fi/cs/publications/2NWGA.html>
16. R.H. Webb, "Confocal optical microscopy," Rep. Prog. Phys. **59**, pp. 427-471, 1996

